

**Finite element method as an alternative to study the electronic structure of confined atoms**Juan-José García-Miranda , Rubicelia Vargas , and Jorge Garza \**Departamento de Química, División de Ciencias Básicas e Ingeniería, Universidad Autónoma Metropolitana-Iztapalapa, San Rafael Atlixco 186, Col. Vicentina, Iztapalapa C.P. 09340, México City, México*

(Received 27 April 2023; accepted 17 August 2023; published 7 September 2023)

The finite element method (FEM) based on a nonregular mesh is used to solve Hartree-Fock and Kohn-Sham equations for three atoms (hydrogen, helium, and beryllium) confined by finite and infinite potentials, defined in terms of piecewise functions or functions with a well-defined first derivative. This approach's reliability is shown when contrasted with Roothaan's approach, which depends on a basis set. Therefore, its exponents must be optimized for each confinement imposed over each atom, which is a monumental task. The comparison between our numerical approach and Roothaan's approach is made by using total and orbital energies from the Hartree-Fock method, where there are several comparison sources. Regarding the Kohn-Sham method, there are few published data and consequently the results reported here can be used as a benchmark for future comparisons. The way to solve Hartree-Fock or Kohn-Sham equations by the FEM is entirely appropriate to study confined atoms with any form of confinement potential. This article represents a step toward developing a fully numerical quantum chemistry code free of basis sets to obtain the electronic structure of many-electron atoms confined by arbitrary confinement.

DOI: [10.1103/PhysRevE.108.035302](https://doi.org/10.1103/PhysRevE.108.035302)**I. INTRODUCTION**

The electronic structure of atoms and molecules suffers important changes when these systems are immersed in environments different from the vacuum. For example, essential differences are observed in the total energy when an atom is under confinement [1–10]. Unfortunately, many computational codes have been designed to study the electronic structure of atoms in the vacuum and consequently they cannot be used when an atom is within an environment different from the gas phase, in particular, when the confinement is modeled by piecewise functions. In this sense, the MEXICA-C code has been designed to study the electronic structure of atoms submitted to several potentials, defined through piecewise functions, that mimic different environments [11–13]. However, this code is based on Roothaan's approach where Hartree-Fock [14] or Kohn-Sham orbitals [15] are represented by a basis set, where functions depend on a set of exponents, which must be adjusted to obtain the minimal energy for each confinement imposed on an atom. The use of functions defined over the whole domain of an atom or molecule is inconvenient since the set of exponents is unique for a particular environment and consequently such a basis set must be reoptimized each time that the system changes its environment [16,17]. Thus, this approach is not recommendable for atoms immersed in an environment different from the vacuum. Alternatively to Roothaan's approach, there are methods based on grids, which avoid the reoptimization of a basis set, which have been used for confined atoms. However, the current implementations are inefficient or limited to studying

one- or two-electron atoms for finite potentials defined in terms of piecewise functions.

The finite element method (FEM) is a powerful numerical approach to solving differential equations. In particular, the FEM has been used to solve the Schrödinger equation for atoms, molecules, and crystals. In principle, this method is versatile to solve differential equations with different boundary conditions. This versatility must also be observed when the Schrödinger equation is solved under different boundary conditions [18–38]. We must mention that there are reports only for two-electron confined atoms analyzed with grid-based methods involving the exact exchange with potentials defined by piecewise functions [32,39]. The main reason for this lack of study is the difficulties presented in implementing the exact exchange within the corresponding algebraic approach.

Regarding the confinement models, defined by piecewise functions, we can mention a relevant potential used to simulate different confinements to represent hard or soft walls. For the first case, an atom is enclosed by a sphere with an infinite potential over its surface and the corresponding wave function or electron density cannot penetrate the potential. In the second case, the sphere's surface imposes a finite potential and the corresponding wave function or electron density can penetrate the region where the potential is defined. Both situations can be represented by

$$v(\mathbf{r}) = \begin{cases} -\frac{Z}{r} & \text{for } r < R_c \\ V_c & \text{for } r \geq R_c, \end{cases} \quad (1)$$

where  $R_c$  represents the radius of the sphere,  $Z$  is the atomic number, and  $V_c$  can be infinite or finite. Atomic units (a.u.) are used throughout this article. For impenetrable walls (infinite potential) the wave function must be canceled at  $R_c$ ; for

\*jgo@xanum.uam.mx

penetrable walls (finite potential) the wave function and its first logarithmic derivative must be continuous at  $R_c$  [40,41]. By looking through the literature on the FEM and its applications to the electronic structure of atoms and molecules in the gas phase, we consider this method appropriate to study atoms and molecules submitted to different potentials that mimic confinements or environments distinct to the vacuum.

Other model potentials, defined by functions with a well-defined first derivative, are used to simulate confinement. For example, the potential

$$W_n(r) = \frac{1}{2}\omega^{n+1}r^{2n}, \quad (2)$$

with  $n = 1$ , can be used to represent several effects, as Bielinska-Waz *et al.* mentioned when they introduced this model potential to simulate confinement [42,43]. For this case, the electronic structure can be obtained by adapting computational codes designed for nonconfined systems. Similarly, models that simulate solvent effects or with Gaussian potentials have been used over standard computational codes to simulate atoms or molecules under extreme pressure [7,44–46].

At this point, it is clear that several ways exist to simulate environments to confine atoms or molecules. In this paper we implement the FEM to solve Hartree-Fock (HF) and Kohn-Sham (KS) equations for atoms confined by different potentials, in particular potentials defined by piecewise functions, to show the convenience of using this grid-based method in studying these systems.

## II. METHODS

In the HF method [14], the wave function  $\Phi(\mathbf{x}_1, \mathbf{x}_2, \dots, \mathbf{x}_N)$  of a system with  $N$  electrons is represented by a Slater determinant

$$\Phi(\mathbf{x}_1, \mathbf{x}_2, \dots, \mathbf{x}_N) = |\chi_i(\mathbf{x}_1)\chi_j(\mathbf{x}_2) \cdots \chi_k(\mathbf{x}_N)|, \quad (3)$$

where each spin orbital has the expression  $\chi(\mathbf{x}) = \phi(\mathbf{r})\sigma(\omega)$ , with  $\sigma = \alpha$  or  $\beta$ . The electronic configuration in a system depends on the combination of orbitals with spin  $\alpha$  or  $\beta$ . The expected value of the energy for this wave function is expressed as

$$\begin{aligned} E_{\text{HF}} = & \sum_{i=1}^N \int d\mathbf{r} \phi_i^* \mathbf{r} \left( -\frac{1}{2}\nabla^2 \right) \phi_i(\mathbf{r}) + \int d\mathbf{r} v(\mathbf{r})\rho(\mathbf{r}) \\ & + \frac{1}{2} \sum_{i=1}^N \sum_{j=1}^N \left( \iint d\mathbf{x} d\mathbf{x}' \frac{\chi_i^*(\mathbf{x})\chi_i(\mathbf{x})\chi_j^*(\mathbf{x}')\chi_j(\mathbf{x}')}{|\mathbf{r} - \mathbf{r}'|} \right. \\ & \left. - \iint d\mathbf{x} d\mathbf{x}' \frac{\chi_i^*(\mathbf{x})\chi_j(\mathbf{x})\chi_j^*(\mathbf{x}')\chi_i(\mathbf{x}')}{|\mathbf{r} - \mathbf{r}'|} \right), \end{aligned} \quad (4)$$

with the electron density  $\rho(\mathbf{r})$  obtained from

$$\rho(\mathbf{r}) = \sum_{i=1}^N \phi_i^*(\mathbf{r})\phi_i(\mathbf{r}). \quad (5)$$

For a closed-shell system, the total energy has the form

$$\begin{aligned} E_{\text{HF}} = & 2 \sum_{i=1}^{N/2} \int d\mathbf{r} \phi_i^* \mathbf{r} \left[ -\frac{1}{2}\nabla^2 + v(\mathbf{r}) \right] \phi_i(\mathbf{r}) \\ & + \frac{1}{2} \iint d\mathbf{r} d\mathbf{r}' \frac{\rho(\mathbf{r})\rho(\mathbf{r}')}{|\mathbf{r} - \mathbf{r}'|} + \mathcal{E}, \end{aligned} \quad (6)$$

with the exact exchange  $\mathcal{E}$  as

$$\mathcal{E} = - \sum_{i=1}^{N/2} \sum_{j=1}^{N/2} \iint d\mathbf{r} d\mathbf{r}' \frac{\phi_i^*(\mathbf{r})\phi_j(\mathbf{r})\phi_j^*(\mathbf{r}')\phi_i(\mathbf{r}')}{|\mathbf{r} - \mathbf{r}'|}. \quad (7)$$

The orbitals  $\{\phi_i(\mathbf{r})\}$  that minimize  $E_{\text{HF}}$  must satisfy the HF equations

$$\begin{aligned} & \left( -\frac{1}{2}\nabla^2 + v(\mathbf{r}) + \int d\mathbf{r}' \frac{\rho(\mathbf{r}')}{|\mathbf{r} - \mathbf{r}'|} - \epsilon_i \right) \phi_i(\mathbf{r}) \\ & = \sum_{j=1}^{N/2} \int d\mathbf{r}' \frac{\phi_j^*(\mathbf{r}')\phi_i(\mathbf{r}')}{|\mathbf{r} - \mathbf{r}'|} \phi_j(\mathbf{r}), \end{aligned} \quad (8)$$

where  $\epsilon_i$  is a Lagrange multiplier representing an HF orbital energy. To solve these equations, it is convenient to use the potentials  $V_\rho(\mathbf{r})$  and  $V_X^{ji}(\mathbf{r})$  to obtain

$$\left[ -\frac{1}{2}\nabla^2 + v(\mathbf{r}) + V_\rho(\mathbf{r}) - \epsilon_i \right] \phi_i(\mathbf{r}) = \sum_{j=1}^{N/2} V_X^{ji}(\mathbf{r})\phi_j(\mathbf{r}), \quad (9)$$

with

$$V_\rho(\mathbf{r}) = \int d\mathbf{r}' \frac{\rho(\mathbf{r}')}{|\mathbf{r} - \mathbf{r}'|}, \quad (10)$$

$$V_X^{ji}(\mathbf{r}) = \int d\mathbf{r}' \frac{\rho_X^{ji}(\mathbf{r}')}{|\mathbf{r} - \mathbf{r}'|}, \quad (11)$$

and

$$\rho_X^{ji}(\mathbf{r}) = \phi_j^*(\mathbf{r})\phi_i(\mathbf{r}). \quad (12)$$

In our implementation of the FEM,  $V_\rho(\mathbf{r})$  and  $V_X^{ji}(\mathbf{r})$  are obtained from the corresponding Poisson equation

$$\nabla^2 V_\rho(\mathbf{r}) = -4\pi\rho(\mathbf{r}), \quad \nabla^2 V_X^{ji}(\mathbf{r}) = -4\pi\rho_X^{ji}(\mathbf{r}), \quad (13)$$

which means we have to apply Poisson's equation for each pair of occupied orbitals.

In the FEM, a differential equation is converted to a variational problem. For this purpose, Eq. (8) is multiplied by a function  $h(\mathbf{r})$  that satisfies the same boundary conditions as the solution and the resulting equation is integrated over the whole space. The next step of the FEM is discretizing the domain where  $\phi$  is defined. Over each element  $\mathbf{e}$  the solution is represented as

$$\phi_i^e(\mathbf{r}) = \sum_{\mu=1}^K c_\mu^i g_\mu^e(\mathbf{r}). \quad (14)$$

Typically,  $\{g_\mu\}$  are polynomials and  $h(\mathbf{r})$  is contained in this set of functions. In this article, Lagrange polynomials are used in the FEM implementation [47]. With this procedure, the

differential equation is converted to the algebraic problem

$$(\mathbf{H}^{\text{core}} + \mathbf{V}_\rho - \epsilon_i \mathbf{S}) \mathbf{c}^i = \sum_{j=1}^{N/2} \mathbf{V}_X^{ji} \mathbf{c}^j, \quad (15)$$

where

$$\mathbf{H}_{v\mu}^{\text{core},e} = \mathbf{T}_{v\mu}^e + \mathbf{V}_{N,v\mu}^e, \quad (16)$$

$$\mathbf{T}_{v\mu}^e = \int d\mathbf{r} g_v^{e*}(\mathbf{r}) \left(-\frac{1}{2} \nabla^2\right) g_\mu^e(\mathbf{r}), \quad (17)$$

$$\mathbf{V}_{N,v\mu}^e = \int d\mathbf{r} g_v^{e*}(\mathbf{r}) v(\mathbf{r}) g_\mu^e(\mathbf{r}), \quad (18)$$

$$\mathbf{V}_{\rho,v\mu}^e = \int d\mathbf{r} g_v^{e*}(\mathbf{r}) V_\rho(\mathbf{r}) g_\mu^e(\mathbf{r}), \quad (19)$$

$$\mathbf{S}_{v\mu}^e = \int d\mathbf{r} g_v^{e*}(\mathbf{r}) g_\mu^e(\mathbf{r}), \quad (20)$$

$$\mathbf{V}_{X,v\mu}^{ji,e} = \int d\mathbf{r} g_v^{e*}(\mathbf{r}) V_X^{ji}(\mathbf{r}) g_\mu^e(\mathbf{r}). \quad (21)$$

Equation (15) cannot be treated as an eigenvalue problem due to the exact exchange involved in the HF equations. An alternative to solving Eq. (15) is the Rayleigh quotient [48]. For this iterative method, we use the following algorithm, where  $\mathbf{x} = \sum_{j=1}^{N/2} \mathbf{V}_X^{ji} \mathbf{c}^j$  and  $\mathbf{F} = \mathbf{H}^{\text{core}} + \mathbf{V}_\rho$ :

**for**  $k = 1$  to  $N$  **do**

$$\epsilon^{(k)} = \mathbf{c}^{(k)T} (\mathbf{F} \mathbf{c}^{(k)} - \mathbf{x}^{(k)}) / \mathbf{c}^{(k)T} \mathbf{S} \mathbf{c}^{(k)}$$

$$(\mathbf{T} - \epsilon^{(k)} \mathbf{S}) \mathbf{w}^{k+1} = \mathbf{x}^{(k)}$$

$$\mathbf{c}^{(k+1)} = \mathbf{w}^{k+1} / \|\mathbf{w}^{k+1}\|$$

**end for**

To solve the self-consistent process, at the beginning of this process we neglect  $V_\rho$  and  $V_X^{ji}$  to obtain the first set of  $\mathbf{C}^i$ . The matrix  $V_\rho$  is built with the first set of vectors, and after a few iterations, the matrix  $V_X^{ji}$  is turned on. As we mentioned above, the Poisson equation is solved for  $V_\rho$  and  $V_X^{ji}$ . For both potentials, the algebraic equation has the form

$$\mathbf{L} \mathbf{v} = \mathbf{f}, \quad (22)$$

with

$$\mathbf{L} = \sum_{e=1}^{Ne} \mathbf{L}_{\mu\nu}^e, \quad (23)$$

$$\mathbf{f} = \sum_{e=1}^{Ne} \mathbf{f}_v^e, \quad (24)$$

$$\mathbf{f}_v^e = \int d\mathbf{r} g_v^{e*}(\mathbf{r}) f(\mathbf{r}), \quad (25)$$

$$\mathbf{L}_{v\mu}^e = \int d\mathbf{r} g_v^e(\mathbf{r}) g_\mu^e(\mathbf{r}). \quad (26)$$

The form of the vector  $\mathbf{f}$  depends on the corresponding potential. For the Hartree potential,  $\mathbf{v} = \mathbf{V}_\rho$  and  $f(\mathbf{r}) = -4\pi \rho(\mathbf{r})$ . For the exchange potential,  $\mathbf{v} = \mathbf{V}_X^{ji}$  and  $f(\mathbf{r}) = -4\pi \rho_X^{ji}(\mathbf{r})$ , with  $\rho_X^{ji}(\mathbf{r})$  defined in Eq. (12). Finally, the solution for each orbital is reached when the total energy changes are lower than  $10^{-10}$  a.u.

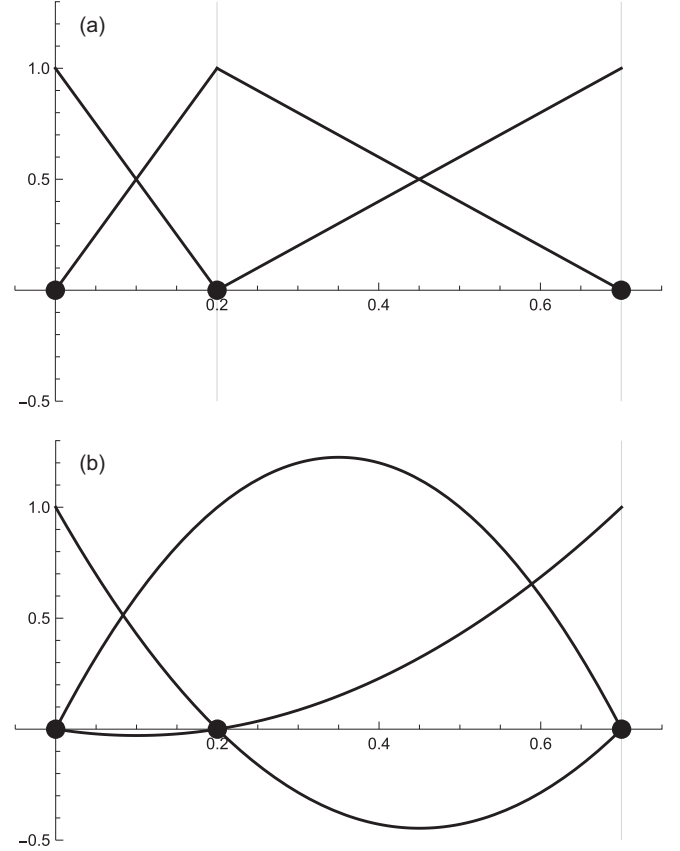


FIG. 1. Nonregular mesh built with three points: (a) two elements with linear polynomials and (b) one element with a quadratic polynomial.

In this article, the implementation of the FEM is in its weak formulation [49]. For each element, the radial part is evaluated by using a Chebyshev quadrature over the interval  $[-1, 1]$  with 200 quadrature points [50]. In our code, the grid used over the radial coordinate has two options: (i) that from Froese-Fischer *et al.* [48],

$$r_i = \frac{e^{(-5+i/32)}}{Z}, \quad (27)$$

and (ii) an exponential one from [35],

$$r_i = (1 + R_\infty)^{i^2/P^\alpha} - 1, \quad (28)$$

where  $R_\infty$  represents the practical infinity and  $P$  the number of grid points.

The mesh from Froese-Fischer *et al.* contains information on the nuclear charge  $Z$  to obtain a dense grid close to the nucleus. The exponential grid is identical for every atom once the value of  $\alpha$  is selected. This grid was tested in a previous work [35] which concluded that  $\alpha = 2$  provides excellent results for free atoms. Our code uses  $\alpha = 2$  as the default. Nevertheless, for a confinement imposed by soft walls,  $\alpha = 3$  presents the best results. In this article, the number of nodes in the mesh is fixed. Thus, the polynomial is adapted to the nodes defined within the mesh. For example, in Fig. 1 a nonregular mesh is defined by three points  $r = 0, 0.2, 0.7$  a.u. In Fig. 1(a) there are linear polynomials. With three nodes, there are two elements of these polynomials. In Fig. 1(b) the three nodes

define quadratic polynomials with only one element. Thus, when we increase the order of a polynomial, the number of nodes does not change. It is worth noting that for the exponential mesh, the number of points is always the same (337 points in our case) independently of the nuclear charge.

Within the KS approach [15], the total energy for a closed-shell system is obtained from

$$E_{\text{KS}} = 2 \sum_{i=1}^{N/2} \int d\mathbf{r} \phi_i^* \mathbf{r} \left[ -\frac{1}{2} \nabla^2 + v(\mathbf{r}) \right] \phi_i(\mathbf{r}) + \frac{1}{2} \iint d\mathbf{r} d\mathbf{r}' \frac{\rho(\mathbf{r})\rho(\mathbf{r}')}{|\mathbf{r} - \mathbf{r}'|} + E_{\text{xc}}[\rho]. \quad (29)$$

This expression is similar to Eq. (6). The  $\mathcal{E}$  energy is the main difference between the HF and KS methods since this term is contained only in the HF method to consider the nonclassical two-electron interactions. Regarding the KS approach, the exact  $E_{\text{xc}}$  functional contains all nonclassical two-electron interactions. In principle, the KS method is exact and the HF method is an approximation. Unfortunately, the exact-exchange correlation functional is unknown; therefore, it is necessary to design approximations of this functional. Some approximations contain  $\mathcal{E}$ , although it is not mandatory. From a practical point of view, the implementation of both methods is essentially the same. However, if  $\mathcal{E}$  is not present in the  $E_{\text{xc}}$  approximation, the KS potential is a local multiplicative potential, which is computationally easier to solve. Thus, if  $V_{\text{xc}}$  is a multiplicative potential, then the KS equations to solve are expressed as

$$\left[ -\frac{1}{2} \nabla^2 + v(\mathbf{r}) + V_{\rho}(\mathbf{r}) + V_{\text{xc}}(\mathbf{r}) - \epsilon_i \right] \phi_i(\mathbf{r}) = 0. \quad (30)$$

If  $\mathcal{E}$  is considered to build  $E_{\text{xc}}$ , as in hybrid exchange-correlation functionals, then the solution of the KS equation will be similar to Eq. (9). Our fully numerical quantum chemistry (FUNQC) code contains the option to use multiplicative or nonmultiplicative potentials, or the mix of both to deal with hybrid exchange-correlation functionals.

Finally, we want to mention an important element for the solution of the HF or KS equations for atoms confined by a finite potential defined by piecewise functions. In this article, the electron-electron interaction  $1/|\mathbf{r}' - \mathbf{r}|$  is neglected within the region  $r \geq R_c$ , since this expression is valid when the electrons are in the vacuum, which is not the case for this region. We are using the proposal by Gorecki and Byers-Brown [51] and followed in other reports [12,52]. Thus, the electron-electron interaction will be overestimated if a screening effect is not considered by the action of the potential [53]. In this article, we impose this restriction on the solution of the corresponding Poisson equation.

### III. RESULTS

#### A. Confined hydrogen atom

The confined hydrogen atom is a system that must be analyzed when new numerical techniques are proposed to solve the corresponding Schrödinger equation since this system admits exact solutions for different confinements [17]. The total energy for the hydrogen atom confined by hard and soft walls is reported in Table I, where the soft walls are represented

TABLE I. Total energy for the hydrogen atom confined by (a) hard walls ( $V_c = \infty$ ) and (b) soft walls ( $V_c = 0.0$ ) and several confinement radii  $R_c$ . All quantities are in atomic units.

$R_c$	Exact <sup>a</sup>	This work		
		Third order	Fourth order	Sixth order
(a)				
0.1	468.99303866	468.99303860	468.99303866	468.99303866
0.1		468.99303860	468.99303935	468.99303858
0.5	14.74797003	14.74797003	14.74797003	14.74797003
0.5		14.74797003	14.74797005	14.74796999
1.0	2.37399087	2.37399087	2.37399087	2.37399087
1.0		2.37399087	2.37399088	2.37399085
3.0	-0.42396729	-0.42396729	-0.42396729	-0.42396729
3.0		-0.42396729	-0.42396729	-0.42396729
5.0	-0.49641701	-0.49641701	-0.49641701	-0.49641701
5.0		-0.49641701	-0.49641701	-0.49641701
20.0	-0.50000000	-0.50000000	-0.50000000	-0.50000000
20.0		-0.50000000	-0.50000000	-0.50000000
(b)				
0.85	-0.04036230	-0.04036230	-0.04036230	-0.04036230
0.85		-0.04036230	-0.04036230	-0.04036230
1.0	-0.12500000	-0.12499999	-0.12500000	-0.12500000
1.0		-0.12500000	-0.12500000	-0.12500000
1.5	-0.33816742	-0.33816739	-0.33816741	-0.33816742
1.5		-0.33816742	-0.33816742	-0.33816742
2.0	-0.43121889	-0.43121885	-0.43121887	-0.43121889
2.0		-0.43121889	-0.43121889	-0.43121889

<sup>a</sup>Results obtained from the methodology of Ref. [17].

by a potential defined by a piecewise function. In this table, the results obtained from our code are contrasted with the corresponding exact values. For this comparison, two meshes were used: The results obtained by the grid from Froese-Fischer *et al.* are reported in the first row and those obtained by the exponential grid are reported in the second row. The impact of the order of the polynomial used in the FEM is also considered in Table I. From these results we observe a good performance of the FEM to describe this atom under several confinements. For strong confinements,  $R_c < 1.0$ , and hard walls, the mesh from Froese-Fischer *et al.* exhibits better results than those obtained from the exponential grid. However, for other confinements, both meshes give the same results. Another important result obtained from this comparison is that the third-order polynomial used in the FEM is enough to obtain results converged to (or slightly different from) those results obtained with a sixth-order polynomial. Thus, for the hydrogen atom confined by hard or soft walls, the FEM with a polynomial of third order is enough and any of the two meshes considered in this article give the same results. It is worth noting that the results obtained for each confinement require only a few seconds in a laptop with an Intel CORE-i5 processor.

#### B. Confined helium atom

The helium atom is the second atom to be considered as a reference since the electron-electron interaction is present. The confined helium atom, in the electron configuration  $1s^2$

TABLE II. (a) Hartree-Fock and (b) Kohn-Sham (LDA) total energies for the helium atom ( $^1S$ ) confined by hard walls ( $V_c = \infty$ ) for several confinement radii  $R_c$ . All quantities are in atomic units.

$R_c$	Other works	Third order	Fourth order	Sixth order	Eighth order
			(a)		
0.1	906.616438 <sup>a</sup>	906.61639647	906.61639659	906.61639660	906.61639653
0.1	906.616349 <sup>b</sup>	906.61639657	906.61639659	906.61639660	906.61639655
0.5	22.790961 <sup>a</sup>	22.79095326	22.79095328	22.79095328	22.79095328
0.5	22.790953 <sup>b</sup>	22.79095328	22.79095328	22.79095328	22.79095328
0.5	22.79095 <sup>c</sup>				
0.5	22.79095 <sup>d</sup>				
1.0	1.061206 <sup>a</sup>	1.06120262	1.06120262	1.06120262	1.06120262
1.0	1.061203 <sup>b</sup>	1.06120262	1.06120262	1.06120262	1.06120262
1.0	1.06120 <sup>c</sup>				
1.0	1.06122 <sup>d</sup>				
1.0	1.06120264 <sup>e</sup>				
2.0	-2.562578 <sup>a</sup>	-2.56258068	-2.56258068	-2.56258068	-2.56258068
2.0	-2.562581 <sup>b</sup>	-2.56258068	-2.56258068	-2.56258068	-2.56258068
2.0	-2.56258 <sup>c</sup>				
2.0	-2.56253 <sup>d</sup>				
2.0	-2.56258073 <sup>e</sup>				
3.0	-2.831047 <sup>a</sup>	-2.83104947	-2.83104947	-2.83104947	-2.83104947
3.0	-2.831050 <sup>b</sup>	-2.83104947	-2.83104947	-2.83104947	-2.83104947
3.0	-2.83105 <sup>c</sup>				
3.0	-2.83083 <sup>d</sup>				
3.0	-2.83104934 <sup>e</sup>				
4.0	-2.858586 <sup>a</sup>	-2.85858879	-2.85858880	-2.85858880	-2.85858880
4.0	-2.858589 <sup>b</sup>	-2.85858879	-2.85858880	-2.85858880	-2.85858880
4.0	-2.85859 <sup>c</sup>				
4.0	-2.85852 <sup>d</sup>				
4.0	-2.85858894 <sup>e</sup>				
10.0	-2.861677 <sup>a</sup>	-2.86167998	-2.86167999	-2.86168000	-2.86168000
10.0	-2.861680 <sup>b</sup>	-2.86167997	-2.86167999	-2.86167999	-2.86167999
10.0	-2.86168 <sup>c</sup>				
			(b)		
0.1		909.07874930	909.07874461	909.07874415	909.07874379
1.0	1.35361 <sup>c</sup>	1.35361776	1.35361707	1.35361701	1.35361698
1.5		-1.64897738	-1.64897780	-1.64897784	-1.64897785
1.6		-1.87830808	-1.87830846	-1.87830849	-1.87830850
2.0	-2.38363 <sup>c,f</sup>	-2.38362974	-2.38362999	-2.38363001	-2.38363002
3.0	-2.68210 <sup>c,f</sup>	-2.68209830	-2.68209837	-2.68209838	-2.68209838
4.0	-2.71813 <sup>c,f</sup>	-2.71812803	-2.71812805	-2.71812805	-2.71812805
10.0	-2.72364 <sup>c,f</sup>	-2.72363973	-2.72363976	-2.72363976	-2.72363976
$\infty$		-2.72363952	-2.72363979	-2.72363979	-2.72363979

<sup>a</sup>Finite element method by Young *et al.* [32].

<sup>b</sup>Roothaan's approach by Young *et al.* [32].

<sup>c</sup>Finite difference method by Martínez-Flores *et al.* [39].

<sup>d</sup>Roothaan's approach by Ludeña [1].

<sup>e</sup>Variational approach by de Morais and Custodio [54].

<sup>f</sup>Roothaan's approach by Aquino *et al.* [55].

( $^1S$ ), is analyzed for hard or soft walls represented by piecewise functions.

### 1. Hard walls

The HF total energy of the helium atom confined by hard walls is reported in Table II. For confinement imposed by hard walls, a fourth-order polynomial gives stable results about the sixth-order polynomial. The impact of the grid on the results is minor. In fact, from a fourth-order polynomial, the

grid from Froese-Fischer *et al.* and exponential grids give the same results. Thus, the two meshes tested in this article and a fourth-order polynomial can be used without problems to study the helium atom confined by hard walls.

There are several reports for the confinement imposed by impenetrable walls, in particular, there is a report where the FEM is applied. Before comparing results obtained by the same technique, it is important to say that there are several differences between the implementation of the FEM in Ref. [32] and our implementation. The evaluation of the electrostatic

potential is the main difference between that work and ours. In Ref. [32] the electrostatic potential was obtained from its integral representation, like the approach used in Ref. [35]. In our implementation, this property was obtained from the solution of Poisson's equation. The grid and the order of the polynomial used in Ref. [32] are different from those used in our implementation; for that reason, we do not expect the same results by the two implementations. However, our results are better than those obtained by the FEM implemented in Ref. [32], which is corroborated in Table II. It is worth noting that our implementation is completely general and the implementation of the FEM in Ref. [32] is *ad hoc* for this atom and it cannot be used for another atom, let us say beryllium.

Recently, Martínez-Flores *et al.* reported a grid-based method to study the helium atom for several confinements [39]. Such a method is based on the finite difference method (FDM) with a nonregular mesh, and this is a good effort to solve the HF equations without a global basis set. Regarding the confinement imposed by hard walls, the FDM gives results similar to those reported by other methodologies and our results are the same as those obtained by this technique, although we must mention that the FDM implemented in Ref. [39] was *ad hoc* to deal with the helium atom and it cannot be applied to another atom in the HF context.

Using Roothaan's approach, there are several reports to solve the HF equations for the helium confined by hard walls. As we have mentioned in the Introduction, this method is based on a basis set that must be optimized for each confinement. In particular, for hard walls, such a basis set must be optimized for each  $R_c$ . From Table II we observe that our implementation of the FEM gives better results than some reported by Roothaan's approach. This is a good conclusion because we are probing whether the FEM is a good alternative to studying confined atoms with a small computational effort and reliable results.

In this article, we deal just with the exchange-only local density approximation (LDA) within the context of the KS approach. We decided to show results related to this exchange-only functional since few data are reported in the literature with this approach. However, the FUNQC code is built so that any exchange-correlation functional can be implemented without any problem.

The total energy obtained by the LDA for the helium confined by hard walls is reported in Table II. For this case, we are using the exponential grid. In the same table we report some results obtained by the finite difference approximation by Martínez-Flores *et al.* [39] and Roothaan's approach by Aquino *et al.* [55]. From these results we observe that the FUNQC results agree with previous reports, although in our case we have reported more figures. It is clear that for extreme confinement radii (small  $R_c$ ) within the KS approach, a polynomial of high order is necessary, which is more pronounced than for the HF approach.

## 2. Soft walls

The solution of the HF equations for this confinement is a challenge for any computational method. Thus, this is a good problem where the FEM will be applied for atoms with more than one electron since the implementation of

the FEM from Ref. [32] was designed only for hard walls. In our study, we observe numerical problems with the grid from Froese-Fischer *et al.*; for that reason we do not use this mesh for this confinement. However, for the exponential grid we do not find problems. Regarding Roothaan's approach, Rodríguez-Bautista *et al.* proposed a basis set defined in two regions, which is a real problem in the evaluation of the two-electron integrals [12], in addition to the problem of the basis set optimization. Thus, the continuity of KS or HF orbitals and their logarithmic derivative is an additional problem with Roothaan's approach. Even with these problems, Rodríguez-Bautista *et al.* implemented in the MEXICA-C code the study of confined many-electron atoms under these circumstances [12].

The HF total energy for helium confined by the finite potential  $V_c = 0.0$  a.u. is reported in Table III. The HF results obtained by our FEM implementation give same results as those obtained by Rodríguez-Bautista *et al.* [12]. Duarte-Alcaráz *et al.* [52] used the same methodology developed by Rodríguez-Bautista *et al.*, although with different basis set. From Table III we observe that our results are slightly better than those reported by Duarte-Alcaráz *et al.* [52]. Marin and Cruz used the direct variational method [41] to tackle this problem and their results show large discrepancies from previous results and ours. Regarding the grid-based methods, Martínez-Flores *et al.* [39] applied the FDM to this problem and we observe some differences from our results. We observe from Table III an important discrepancy between the results obtained in this article and those obtained by the FDM for  $R_c = 0.6$  and  $2.0$  a.u., since for these confinement radii the FDM predicts lower results than those reported by us and by Roothaan's approach. In our opinion, the FDM overestimates the total energy for these  $R_c$  values. We admit that this type of confinement does impose numerical problems for small confinement radii. Thus, the FEM is a good alternative for this kind of problem.

The KS (LDA) results are also in Table III. Here the FEM results are reported for the helium atom for this confinement. We observe that the order of the polynomial is crucial for this confinement for small confinement radii. In fact, this observation is valid also for the solution of the HF equations. This is an important conclusion of this article: Polynomials of high order are necessary for the description of atoms confined by soft walls for the HF and KS approaches.

From the comparison of the HF and LDA results from Table III, it is interesting that the LDA predicts a total energy lower than the HF results for small confinement radii. It is well known that the exchange-only LDA underestimates the total energy with respect to the HF results for atoms and molecules when these systems do not exhibit spatial restrictions. For this case we observe that  $E_{LDA} < E_{HF}$  for  $R_c \leq 1.0$  a.u. This result suggests that systems under high pressure could be described erroneously by the exchange-only LDA functional since for some regions this approximation overestimates or underestimates the total energy with respect to HF results.

## 3. Orbital energy

The behavior of the orbital energy  $\epsilon_{1s}$  for the helium atom confined by hard walls and soft walls is presented in Fig. 2.

TABLE III. (a) Hartree-Fock and (b) Kohn-Sham (LDA) total energies for the helium atom ( $1S$ ) confined by soft walls ( $V_c = 0.0$ ) for several confinement radii  $R_c$ . All quantities are in atomic units.

$R_c$	Other works	Third order	Fourth order	Sixth order	Eighth order
			(a)		
0.5	-0.64040 <sup>a</sup>	-0.64084457	-0.64084309	-0.64084218	-0.64084176
0.5	-0.6408 <sup>b</sup>				
0.5	-0.2412 <sup>c</sup>				
0.6	-1.19434 <sup>a</sup>	-1.19418681	-1.19418486	-1.19418363	-1.19418308
0.6	-1.19418 <sup>c</sup>				
1.0	-2.34740 <sup>a</sup>	-2.34764887	-2.34764756	-2.34764679	-2.34764645
1.0	-2.3476 <sup>b</sup>				
1.0	-2.0522 <sup>c</sup>				
1.0	-2.34751 <sup>d</sup>				
2.0	-2.82554 <sup>a</sup>	-2.82542162	-2.82542169	-2.82542162	-2.82542159
2.0	-2.8254 <sup>b</sup>				
2.0	-2.6184 <sup>c</sup>				
2.0	-2.82537 <sup>d</sup>				
3.0	-2.85882 <sup>a</sup>	-2.85881502	-2.85881522	-2.85881522	-2.85881522
3.0	-2.8588 <sup>a</sup>				
3.0	-2.7579 <sup>c</sup>				
4.0	-2.86146 <sup>a</sup>	-2.86145786	-2.86145833	-2.86145834	-2.86145834
4.0	-2.8615 <sup>a</sup>				
4.0	-2.8054 <sup>c</sup>				
10.0	-2.86168 <sup>a</sup>	-2.86167973	-2.86167999	-2.86168000	-2.86168000
10.0	-2.86168 <sup>c</sup>				
$\infty$	-2.86167999 <sup>e</sup>	-2.86167985	-2.86167999	-2.86167999	-2.86167999
			(b)		
0.5	-0.24447 <sup>a</sup>	-0.89080572	-0.89080452	-0.89080378	-0.89080345
0.6	-1.43234 <sup>a</sup>	-1.43302970	-1.43302804	-1.43302701	-1.43302656
1.0	-2.40088 <sup>a</sup>	-2.40106346	-2.40106216	-2.40106141	-2.40106107
2.0	-2.70977 <sup>a</sup>	-2.70971914	-2.70971912	-2.70971902	-2.70971897
3.0	-2.72290 <sup>a</sup>	-2.72289773	-2.72289790	-2.72289789	-2.72289789
4.0	-2.72360 <sup>a</sup>	-2.72359632	-2.72359688	-2.72359688	-2.72359688
10.0	-2.72364 <sup>a</sup>	-2.72363935	-2.72363979	-2.72363979	-2.72363979
$\infty$		-2.72363952	-2.72363979	-2.72363979	-2.72363979

<sup>a</sup>Finite difference method by Martínez-Flores *et al.* [39].

<sup>b</sup>Roothaan's approach by Rodríguez-Bautista *et al.* [12].

<sup>c</sup>Variational method by Marin and Cruz [41].

<sup>d</sup>Roothaan's approach by Duarte-Alcaráz *et al.* [52].

<sup>e</sup>Pseudospectral method to solve Hartree-Fock equations by Cinal [56].

The plot shows the HF (dotted line) and KS (LDA) (solid line) results.

As in other reports, the confinement imposed by hard walls increases rapidly the orbital energy as shown in Fig. 2(a). We observe that for all  $R_c$  considered in this work, the orbital energy obtained by the HF method is always less than that obtained by the KS (LDA) method. For example, for  $R_c = 0.1$  a.u. the hard-wall confinement produces  $\epsilon_{1s}^{\text{HF}} = 462.329\,249\,07$  a.u. and  $\epsilon_{1s}^{\text{LDA}} = 469.978\,954\,94$  a.u. For large values of  $R_c$  the relationship  $\epsilon_{1s}^{\text{HF}} < \epsilon_{1s}^{\text{LDA}}$  is also valid. Thus, for this confinement the orbital energy  $\epsilon_{1s}^{\text{LDA}}$  reaches zero for a larger confinement radius with regard to  $\epsilon_{1s}^{\text{HF}}$ .

The behavior of  $\epsilon_{1s}$  when the helium atom is submitted to the confinement imposed by soft walls is quite different from that observed for hard walls. In particular, for KS (LDA) results we observe a region where the orbital energy is lower than that obtained for the free atom. Thus, there is a confine-

ment region where this exchange functional binds an electron with a higher strength to that imposed by the nucleus. We must take into account that this exchange functional is an approximation to the HF method since its analytical expression is obtained from the exact exchange evaluated with plane waves for the electron gas model. Therefore, we conclude that the results obtained from the KS (LDA) method are incorrect when the helium atom is confined by soft walls. Another anomaly presented by the KS (LDA) functional is that  $\epsilon_{1s}^{\text{LDA}} < \epsilon_{1s}^{\text{HF}}$  for small confinement radii. Such behavior is evidenced in Fig. 2(b) for  $R_c \leq 0.6$  a.u., where  $\epsilon_{1s}^{\text{LDA}} = -0.369\,156\,29$  a.u. and  $\epsilon_{1s}^{\text{HF}} = -0.366\,535\,78$  a.u. This result is consistent with the behavior delivered by the total energy, as it was discussed previously. Duarte-Alcaráz *et al.* [52] found similar results comparing the Perdew-Burke-Ernzerhof (PBE) exchange functional with the HF one. Because the local part of the PBE exchange is related directly to the LDA, we conclude that the electron gas model is responsible of the anomalous

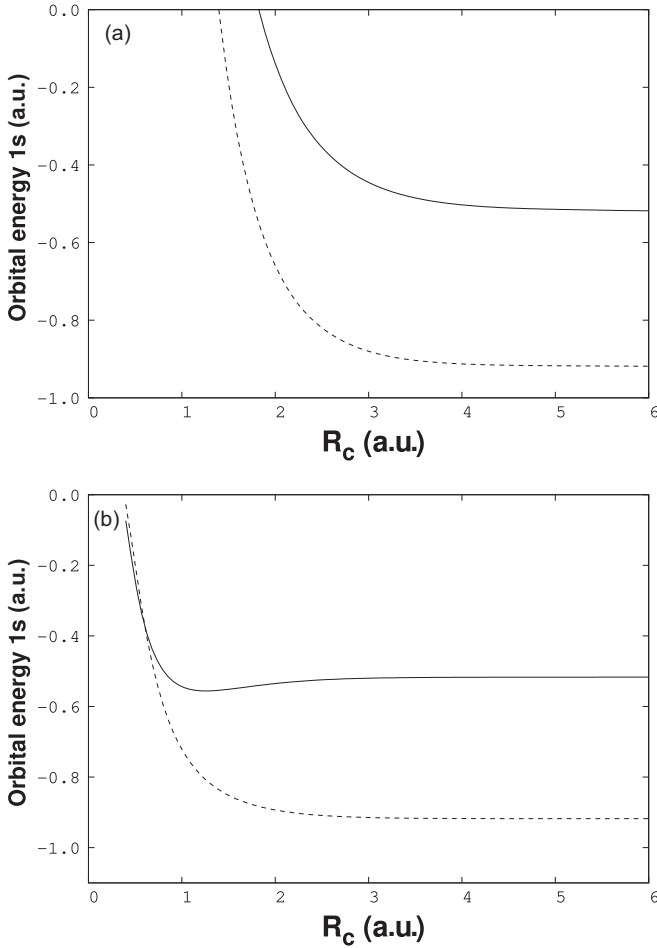


FIG. 2. Orbital energy  $\epsilon_{1s}$  for the helium atom confined by (a) hard walls and (b) soft walls. The solid line shows the Kohn-Sham (LDA) results and the dotted line the Hartree-Fock results..

behavior of the total and orbital energy for the helium confined by soft walls.

#### 4. Electron density and cusp condition

It is recognized that the Kato cusp condition measures the quality of the electron density delivered by a numerical method [57]. The electron density evaluated at the nucleus,  $\rho(0)$ , and the Kato cusp condition of the helium confined by hard and soft walls are reported in Table IV. For this table an eighth-order polynomial was used to solve the HF and KS equations. Comparing our results with those obtained by Roothaan's approach from Young *et al.* [32] for hard-wall confinement, it is clear that there are discrepancies mainly for small confinement radii. However, for moderate and large confinement radii the results coincide for the precision reported by Young *et al.* [32]. Additionally, from this table we observe that for hard walls the electron density grows rapidly for small confinement radii and always  $\rho(0)_{\text{HF}} > \rho(0)_{\text{LDA}}$ . However, such an observation is not valid for soft-wall confinement since for small confinement radii ( $R_c \leq 0.6$  a.u.)  $\rho(0)_{\text{HF}} < \rho(0)_{\text{LDA}}$ . Recall that precisely in this region  $E_{\text{LDA}} < E_{\text{HF}}$ . Thus, an overestimation of the total energy is associated with localization of the electron density around the nucleus.

TABLE IV. Hartree-Fock and Kohn-Sham (LDA) electron densities evaluated at the nucleus (first row) and for the Kato cusp condition (second row) for the helium atom's confined (a) hard walls ( $V_c = \infty$ ) and (b) soft walls ( $V_c = 0.0$ ) for several confinement radii. An eighth-order polynomial was used for the FEM. The electron density and confinement potential are in atomic units.

$R_c$	Other works	HF	KS (LDA)
		(a)	
0.1	3551.5382 <sup>a</sup>	3551.54389339	3542.83735847
0.1		1.00000002	1.00000002
0.5	46.6137 <sup>a</sup>	46.61363410	46.12752171
0.5		1.00000001	1.00000000
1.0	10.8554 <sup>a</sup>	10.85533586	10.67503534
1.0		1.00000000	1.00000000
2.0	4.4896 <sup>a</sup>	4.48958974	4.39104893
2.0		1.00000000	1.00000000
3.0	3.7362 <sup>a</sup>	3.73622547	3.63544703
3.0		1.00000000	1.00000000
4.0	3.6157 <sup>a</sup>	3.61570815	3.50224511
4.0		1.00000000	1.00000000
10.0	3.5959 <sup>a</sup>	3.59591828	3.47352682
10.0		1.00000000	1.00000000
		(b)	
0.5		5.16263206	5.71446360
0.5		1.00000001	1.00000002
0.6		5.57794063	5.63475717
0.6		1.00000002	1.00000002
1.0		4.68752643	4.35311665
1.0		1.00000001	1.00000003
2.0		3.73704044	3.54024561
2.0		1.00000001	1.00000001
3.0		3.61251572	3.47845431
3.0		1.00000002	1.00000001
4.0		3.59763316	3.47389051
4.0		1.00000001	1.00000002
10.0		3.59591826	3.47352643
10.0		1.00000001	1.00000002
$\infty$	3.59591826 <sup>b</sup>	3.59591826	3.47352643
$\infty$		0.99999999	0.99999999

<sup>a</sup>Roothaan's approach to solve HF equations by Young *et al.* [32].

<sup>b</sup>Pseudospectral method to solve Hartree-Fock equations by Cinal [56].

Evidently, the FUNQC code gives electron densities that satisfy the Kato cusp condition, as observed from Table IV.

Unfortunately, there are no reports of  $\rho(0)$  and its Kato cusp condition for the helium confined by soft walls. From Table IV it is evident that its behavior is different from that observed by a confinement imposed by hard walls since it does not present large values for small confinement radii. In our opinion, these values represent a benchmark for these properties and they must be contrasted with new numerical methodologies proposed in the future.

#### C. Beryllium atom

This atom is quite interesting since it reacts appreciably when this is confined. For this atom, only Roothaan's approach has been used to describe its electronic structure for

TABLE V. (a) Hartree-Fock and (b) Kohn-Sham (LDA) total energies for the beryllium atom ( $^1S$ ) confined by (i) hard ( $V_c = \infty$ ) and (ii) soft walls ( $V_c = 0.0$ ) for several confinement radii  $R_c$ . All quantities are in atomic units.

$R_c$	Other works	Third order	Fourth order	Sixth order	Eighth order
			(a)		
			(i)		
1.00	+9.7327 <sup>a</sup>	9.73244879	9.73244882	9.73244882	9.73244882
1.00	+9.73244913 <sup>b</sup>				
1.50	-6.9477 <sup>a</sup>	-6.94774905	-6.94774903	-6.94774903	-6.94774903
1.50	-6.94774833 <sup>b</sup>				
1.60	-8.3128 <sup>c</sup>	-8.31285087	-8.31285086	-8.31285086	-8.31285086
2.00	-11.5079 <sup>a</sup>	-11.50791883	-11.50791883	-11.50791883	-11.50791883
2.00	-11.5078 <sup>c</sup>				
2.00	-11.50791716 <sup>b</sup>				
2.50	-13.1583 <sup>a</sup>	-13.15833966	-13.15833967	-13.15833967	-13.15833967
2.50	-13.1583 <sup>c</sup>				
2.50	-13.15833850 <sup>b</sup>				
3.00	-13.8631 <sup>a</sup>	-13.86308324	-13.86308326	-13.86308326	-13.86308326
3.00	-13.8631 <sup>c</sup>				
3.00	-13.86308240 <sup>b</sup>				
4.00	-14.3685 <sup>a</sup>	-14.36869053	-14.36869057	-14.36869057	-14.36869057
4.00	-14.3678 <sup>c</sup>				
4.00	-14.36869002 <sup>b</sup>				
10.00	-14.5729 <sup>c</sup>	-14.57287714	-14.57287728	-14.57287728	-14.57287728
10.00	-14.57287734 <sup>b</sup>				
			(ii)		
1.5	-13.64448 <sup>d</sup>	-13.64448888	-13.64448897	-13.64448855	-13.64448838
1.75	-13.84892 <sup>d</sup>	-13.84896533	-13.84896511	-13.84896433	-13.84896397
2.0	-14.0440 <sup>c</sup>	-14.04398788	-14.04398942	-14.04398867	-14.04398834
2.0	-14.04390 <sup>d</sup>				
2.5	-14.2994 <sup>c</sup>	-14.29993060	-14.29993078	-14.29993030	-14.29993007
2.5	-14.29958 <sup>d</sup>				
3.0	-14.4312 <sup>c</sup>	-14.43123375	-14.43123410	-14.43123380	-14.43123368
3.0	-14.43080 <sup>d</sup>				
6.0	-14.56995 <sup>d</sup>	-14.56998441	-14.56998645	-14.56998647	-14.56998646
8.0	-14.57281 <sup>d</sup>	-14.57281024	-14.57281173	-14.57281176	-14.57281177
10.0	-14.5730 <sup>c</sup>	-14.57300824	-14.57300988	-14.57300990	-14.57300990
10.0	-14.57301 <sup>d</sup>				
$\infty$	-14.57302317 <sup>e</sup>	-14.57302214	-14.57302317	-14.57302317	-14.57302317
$\infty$	-14.57302317 <sup>f</sup>				
			(b)		
			(i)		
1.0		10.1829200379	10.1829136032	10.1829131602	10.1829130108
1.5		-6.5619751045	-6.5619795088	-6.5619797912	-6.5619798746
1.6		-7.9335653187	-7.9335694242	-7.9335696846	-7.9335697604
2.0		-11.1443787074	-11.1443818411	-11.1443820337	-11.1443820881
2.5		-12.8022667362	-12.8022690156	-12.8022691524	-12.8022691916
3.0		-13.5092846638	-13.5092863473	-13.5092864471	-13.5092864775
4.0		-14.0158557802	-14.0158567164	-14.0158567715	-14.0158567918
10.0		-14.2230512950	-14.2230514803	-14.2230514817	-14.2230514824
			(ii)		
1.5		-13.2508055128	-13.2501707729	-13.2497807363	-13.2413719559
1.75		-13.5947773763	-13.5947785351	-13.5947778424	-13.5947774931
2.0		-13.8245673076	-13.8245690980	-13.8245683972	-13.8245680661
2.5		-14.0416955746	-14.0416959902	-14.0416955219	-14.0416953121
3.0		-14.1403194831	-14.1403200188	-14.1403197059	-14.1403193401
6.0		-14.2225251199	-14.2225273774	-14.2225273743	-14.2225273694

TABLE V. (*Continued.*)

$R_c$	Other works	Third order	Fourth order	Sixth order	Eighth order
8.0		-14.2232567395	-14.2232584874	-14.2232585092	-14.2232585163
10.0		-14.2232874275	-14.2232894729	-14.2232894904	-14.2232894906
$\infty$		-14.2232895018	-14.2232908248	-14.2232908295	-14.2232908295

<sup>a</sup>Roothaan's approach to solve HF equations by Ludeña [1].

<sup>b</sup>Variational approach by de Moraes and Custodio [54].

<sup>c</sup>Roothaan's approach to solve HF equations by Rodriguez-Bautista *et al.* [12].

<sup>d</sup>Roothaan's approach to solve HF equations by Duarte-Alcaraz *et al.* [52].

<sup>e</sup>Pseudospectral method to solve HF equations by Cinal [56].

<sup>f</sup>FEM to solve HF and KS equations by Lehtola [35].

hard or soft confinement. Thus, this confined atom is analyzed here by a free-basis set method, in particular, by the FEM. The total energy of the beryllium atom with the configuration  $1s^2 2s^2$  ( $^1S$ ) obtained by our FEM implementation is reported in Table V and this is contrasted with some results obtained by Roothaan's approach [1,12,52]. It is important to insist that Roothaan's approach requires exponents in the basis set. The optimization of such exponents is a very expensive computational task.

Analyzing the Hartree-Fock results, in Table V we observe that for the confinement imposed by hard walls there is a rapid convergence of the total energy obtained by the FEM with regard to the order of the polynomial, where the fourth order gives good estimations of the total energy for this confined atom. It is remarkable that the FEM results are better than those reported for Roothaan's method used with two different basis sets. Thus, the results reported in this article can be used as a benchmark for the confined beryllium atom. Regarding the beryllium atom confined by soft walls, the convergence observed for the total energy with regard to the order of the polynomial is not the same for this confinement with respect to the confinement by hard walls. For this reason, a high-order polynomial is necessary to deal with this atom for the confinement imposed by soft walls, which is a conclusion obtained also for the helium atom under these circumstances. Comparing the FEM results with those obtained by Roothaan's approach, we found some confinements where the FEM is superior. However, we must remark that the response from the FEM takes a few seconds, whereas for Roothaan's approach the basis set optimization takes a great deal of time and consequently this approach is computationally expensive. Thus, the FEM is a good alternative to study atoms under several confinements.

The KS (LDA) results reported in Table V are different. From this table it is clear that for this approach it is necessary to use high-order polynomials. However, even for high-order polynomial the computational effort is low. In our opinion, these results can be useful as a benchmark for new numerical proposals to solve KS equations with spatial restrictions. Finally,  $\rho(0)$  and the Kato cusp condition for the beryllium atom confined by hard and soft walls are reported in Table VI. For this atom there are no anomalies presented for the helium atom and always  $\rho_{\text{HF}}(0) > \rho_{\text{LDA}}(0)$ . For hard walls,  $\rho(0)$  is increased when  $R_c$  takes small values. However, for the

TABLE VI. Hartree-Fock and Kohn-Sham (LDA) electron densities evaluated at the nucleus,  $\rho(0)$ , and for the Kato cusp condition for the beryllium atom confined by (a) hard walls ( $V_c = \infty$ ) and (b) soft walls ( $V_c = 0.0$ ) for several confinement radii. An eighth-order polynomial was used for the FEM. The electron density and confinement potential are in atomic units.

$R_c$	Other works	HF	LDA
		(a)	
1.0		81.82131846	80.78778607
1.0		1.00000000	1.00000000
1.5		51.36534495	50.54630657
1.5		1.00000000	1.00000000
1.6		48.71973322	47.91792879
1.6		1.00000000	1.00000000
2.0		42.30848951	41.54407638
2.0		1.00000000	1.00000000
2.5		38.81141215	38.06548505
2.5		1.00000000	1.00000000
3.0		37.24306629	36.50948288
3.0		1.00000000	1.00000000
4.0		36.02852439	35.31604862
4.0		1.00000000	1.00000000
10.0		35.38896539	34.70171862
10.0		0.99999999	1.00000000
		(b)	
1.5		35.60806974	33.81031661
1.5		1.00000001	1.00000001
1.75		36.33379056	35.85519414
1.75		1.00000001	1.00000001
2.0		36.39444590	35.68011353
2.0		1.00000001	1.00000001
2.5		36.06603022	35.26443309
2.5		1.00000001	1.00000001
3.0		35.80183277	35.00361644
3.0		1.00000001	1.00000000
6.0		35.40503351	34.70524871
6.0		1.00000001	1.00000001
8.0		35.38935804	34.70035518
8.0		1.00000001	1.00000001
10.0		35.38784681	34.70008913
10.0		1.00000001	1.00000001
$\infty$	35.38771674110 <sup>a</sup>	35.38771674	34.70007506
$\infty$		0.999999993	0.999999994

<sup>a</sup>Pseudospectral method to solve HF equations by Cinal [56].

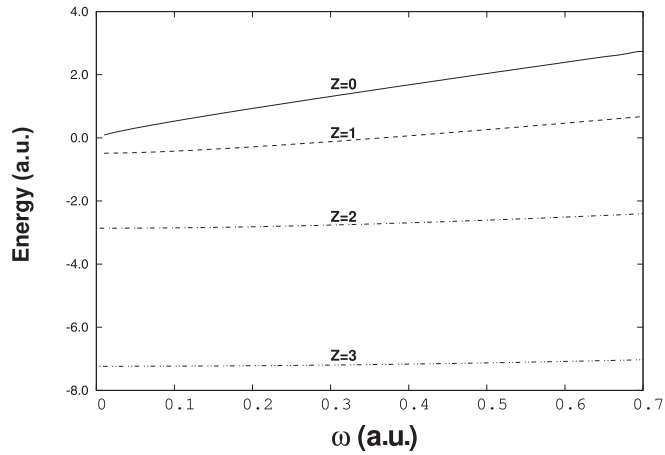


FIG. 3. Hartree-Fock total energy for two-electron atoms confined by the potential  $W_1 = \frac{1}{2}\omega^2 r^2$  for atoms with different nuclear charge  $Z$ .

confinement imposed by soft walls there is a confinement region where the electron density is localized close to the nucleus giving a maximum of  $\rho(0)$ . This result is valid for both the HF and KS (LDA) methods.

#### D. Confinement imposed by a harmonic potential

The harmonic potential has been used to confine atoms and molecules. By its nature, this potential can be incorporated relatively easily in codes based on Slater or Gaussian functions to represent HF or KS orbitals. As we have mentioned in this article, the FEM is quite versatile to solve HF or KS equations. In particular, for potentials defined in Eq. (2), its implementation is very simple. The HF total energy for

two-electron atoms with the configuration  $1s^2$  is presented in Fig. 3. The results of Fig. 3 can be compared with those plots reported by Bielinska-Waz *et al.* [42]. Such a comparison is not exact since the results in Ref. [42] were obtained from the correlated method's configuration interaction. Therefore, our results are above those reported by Bielinska-Waz *et al.*, although our results exhibit the same behavior delivered by the correlated method. Results found by our FEM implementation are reported in Table VII. These results are contrasted with those results obtained from MEXICA-C code using three different basis sets, specifically those from Clementi and Roetti [58], Bunge *et al.* [59], and Koga *et al.* [60]. These basis sets were optimized to use Slater-type orbitals for free atoms. This article used the corresponding basis set designed for the helium atom for the hydride ion. We must mention that all implementations of the confinement imposed by the harmonic potential in codes based on basis set functions use the basis sets designed for free atoms. The results obtained by the three basis sets are reported in Table VII. This comparison shows that the three basis sets considered in this article give HF total energies above the results estimated by our FEM implementation. This observation corroborates the results mentioned in the Introduction: If a basis set is used to study confined systems, then such a basis set must be optimized for the confinement imposed. With this observation, we suggest that all calculations reported for confined systems by harmonic potentials must be revisited to test the impact of the basis set on the reported results. For our discussion, we observe a difference of 0.19 a.u. (119.98 kcal/mol) between the results obtained from the basis sets of Koga *et al.* and Bunge *et al.* for the Be atom and  $\omega = 1.0$  a.u. It is worth noting that the basis set from Koga *et al.* was designed to get the best total energy and satisfy some wave-function properties such as the

TABLE VII. Hartree-Fock total energy for atoms confined by the harmonic potential  $W_1 = \frac{1}{2}\omega^2 r^2$ . Results in the fourth column were obtained using eighth-order polynomials.

$\omega$	Clementi and Roetti <sup>a</sup>	Bunge <i>et al.</i> <sup>b</sup>	Koga <i>et al.</i> <sup>c</sup>	FUNQC
H <sup>-</sup>				
0.2	-0.23937076	-0.24794176	-0.28483591	-0.28544318
0.4	0.06729260	0.06609749	0.06864058	0.06389895
0.6	0.48545799	0.47895270	0.46711497	0.46523991
He				
0.2	-2.81544799	-2.81554321	-2.81592590	-2.81593280
0.4	-2.68854519	-2.68954291	-2.69181420	-2.69195250
0.6	-2.50486912	-2.50720761	-2.50927756	-2.51068594
Li <sup>+</sup>				
0.2	-7.21869241	-7.21869372	-7.21869395	-7.23530227
0.4	-7.16653556	-7.16654448	-7.16654539	-7.16654566
0.6	-7.08249366	-7.08252456	-7.08253290	-7.08253437
Be				
0.2	-14.29660455	-14.29451804	-14.29773456	-14.29836511
0.4	-13.70656154	-13.69856651	-13.70731445	-13.71051865
0.6	-12.94888570	-12.87378951	-12.95805790	-12.96077544
0.8	-12.03653792	-11.91864778	-12.08533531	-12.10213223
1.0	-11.00897304	-10.93607421	-11.12727584	-11.16148999

<sup>a</sup>Roothaan's approach using the basis set of Clementi and Roetti [58].

<sup>b</sup>Roothaan's approach using the basis set of Bunge *et al.* [59].

<sup>c</sup>Roothaan's approach using the basis set of Koga *et al.* [60].

cuspid condition. Consequently, large basis sets were reported by Koga *et al.* This is why this basis set gives results close to those obtained by the FEM. In this comparison, MEXICA-C and FUNQC spend similar computational time to get convergence in the self-consistent process. However, we will need many calculations for Roothaan's approach if we want an optimized basis set. This is an example of the aim of this article: The FEM is convenient for studying systems submitted to different confinements without loss of accuracy.

#### IV. CONCLUSION

In this article the fully numerical quantum chemistry code was developed to solve Hartree-Fock and Kohn-Sham equations for atoms confined by impenetrable or penetrable walls through a model potential. The FUNQC code solves HF or KS equations by using the finite element method, where polynomials of different order are used to solve algebraic

equations associated with Poisson's equations. The benefits of the finite element method were observed for atoms confined by spatial restrictions since this method is quite versatile to impose different boundary conditions, particularly for potentials defined by piecewise functions. The implementation is numerically stable and reliable when previous results of hydrogen, helium, and beryllium atoms are contrasted with the results delivered by our proposal. The implementation of the same methodology to solve HF and KS equations for many-electron diatomic molecules is left for future work. This is the first step to building a code free of global basis sets to study atoms and molecules spatially confined.

#### ACKNOWLEDGMENTS

J.-J.G.-M. is grateful to CONACYT, México, for financial support through a Ph.D. scholarship, Grant No. 467603.

- 
- [1] E. V. Ludeña, *J. Chem. Phys.* **69**, 1770 (1978).
- [2] J. Garza, R. Vargas, and A. Vela, *Phys. Rev. E* **58**, 3949 (1998).
- [3] J. P. Connerade, V. K. Dolmatov, and P. A. Lakshmi, *J. Phys. B* **33**, 251 (2000).
- [4] C. Díaz-García and S. A. Cruz, *Int. J. Quantum Chem.* **108**, 1572 (2008).
- [5] *Advances in Quantum Chemistry: Theory of Confined Quantum Systems*, edited by J. R. Sabin and E. J. Brändas (Elsevier, Amsterdam, 2009), Vols. 57 and 58.
- [6] *Electronic Structure of Quantum Confined Atoms and Molecules*, edited by K. D. Sen (Springer, Cham, 2014).
- [7] R. Cammi, *J. Comput. Chem.* **36**, 2246 (2015).
- [8] E. Ley-Koo, *Rev. Mex. Fis.* **64**, 326 (2018).
- [9] J. J. García-Miranda, J. Garza, I. A. Ibarra, A. Martínez, M. A. Martínez-Sánchez, M. Rivera-Almazo, and R. Vargas, in *Chemical Reactivity in Confined Systems: Theory, Modelling and Applications*, edited by P. K. Chattaraj and D. Chakraborty (Wiley, New York, 2021), Chap. 4, pp. 69–79.
- [10] W. S. Nascimento, M. M. de Almeida, and F. V. Prudente, *Eur. Phys. J. D* **75**, 171 (2021).
- [11] J. Garza, J.-M. Hernández-Pérez, J.-Z. Ramírez, and R. Vargas, *J. Phys. B* **45**, 015002 (2012).
- [12] M. Rodríguez-Bautista, C. Díaz-García, A. M. Navarrete-López, R. Vargas, and J. Garza, *J. Chem. Phys.* **143**, 034103 (2015).
- [13] M.-A. Martínez-Sánchez, M. Rodríguez-Bautista, R. Vargas, and J. Garza, *Theor. Chem. Acc.* **135**, 207 (2016).
- [14] A. Szabo and N. S. Ostlund, *Modern Quantum Chemistry: Introduction to Advanced Electronic Structure Theory* (Dover, New York, 1996).
- [15] R. G. Parr and W. Yang, *Density-Functional Theory of Atoms and Molecules* (Oxford University Press, Oxford, 1994).
- [16] J. Garza and R. Vargas, *Adv. Quantum Chem.* **57**, 241 (2009).
- [17] M.-A. Martínez-Sánchez, R. Vargas, and J. Garza, in *Asymptotic Behavior: An Overview*, edited by S. P. Riley (NOVA, Hauppauge, 2020), Chap. 3, pp. 101–132.
- [18] D. Heinemann, D. Kolb, and B. Fricke, *Chem. Phys. Lett.* **137**, 180 (1987).
- [19] D. Heinemann, B. Fricke, and D. Kolb, *Chem. Phys. Lett.* **145**, 125 (1988).
- [20] D. Heinemann, B. Fricke, and D. Kolb, *Phys. Rev. A* **38**, 4994 (1988).
- [21] D. Sundholm, J. Olsen, P.-Å. Malmqvist, and B. O. Roos, in *Numerical Determination of the Electronic Structure of Atoms, Diatomic and Polyatomic Molecules*, edited by M. Defranceschi and J. Delhalle, NATO Advanced Studies Institute, Series C: Mathematical and Physical Sciences (Kluwer, Dordrecht, 1989), Vol. 271, pp. 329–334.
- [22] D. Sundholm and J. Olsen, *Chem. Phys. Lett.* **198**, 526 (1992).
- [23] D. Sundholm and J. Olsen, *J. Phys. Chem.* **96**, 627 (1992).
- [24] L. Yang, D. Heinemann, and D. Kolb, *Phys. Rev. A* **48**, 2700 (1993).
- [25] J. Kobus, L. Laaksonen, and D. Sundholm, *Comput. Phys. Commun.* **98**, 346 (1996).
- [26] M. Tokman, D. Sundholm, and P. Pyykko, *Chem. Phys. Lett.* **291**, 414 (1998).
- [27] A. von Kopylow, D. Heinemann, and D. Kolb, *J. Phys. B* **31**, 4743 (1998).
- [28] W. Zheng and L. Ying, *Int. J. Quantum Chem.* **97**, 659 (2004).
- [29] R. Alizadegan, K. J. Hsia, and T. J. Martinez, *J. Chem. Phys.* **132**, 034101 (2010).
- [30] P. E. Grabowski and D. F. Chernoff, *Phys. Rev. A* **81**, 032508 (2010).
- [31] M. Braun, *J. Comput. Appl. Math.* **270**, 100 (2014).
- [32] T. D. Young, R. Vargas, and J. Garza, *Phys. Lett. A* **380**, 712 (2016).
- [33] V. I. Pupyshev and H. E. Montgomery, Jr., *Theor. Chem. Acc.* **136**, 138 (2017).
- [34] S. Lehtola, *Int. J. Quantum Chem.* **119**, e25944 (2019).
- [35] S. Lehtola, *Int. J. Quantum Chem.* **119**, e25945 (2019).
- [36] S. Lehtola, *Int. J. Quantum Chem.* **119**, e25968 (2019).
- [37] M. Braun and K. O. Obodo, *Eur. Phys. J. B* **92**, 230 (2019).
- [38] L. Zhu, Y. Y. He, L. G. Jiao, Y. C. Wang, and Y. K. Ho, *Int. J. Quantum Chem.* **120**, e26245 (2020).
- [39] C. Martínez-Flores, M.-A. Martínez-Sánchez, R. Vargas, and J. Garza, *Eur. Phys. J. D* **75**, 100 (2021).

- [40] E. Ley-Koo and S. Rubinstein, *J. Chem. Phys.* **71**, 351 (1979).
- [41] J. L. Marin and S. A. Cruz, *J. Phys. B* **25**, 4365 (1992).
- [42] D. Bielinska-Waz, J. Karwowski, and G. H. F. Diercksen, *J. Phys. B* **34**, 1987 (2001).
- [43] L. F. Pasteka, T. Helgaker, T. Saue, D. Sundholm, H. J. Werner, M. Hasanbulli, J. Major, and P. Schwerdtfeger, *Mol. Phys.* **118**, e1730989 (2020).
- [44] M. Scheurer, A. Dreuw, E. Epifanovsky, M. Head-Gordon, and T. Stauch, *J. Chem. Theory Comput.* **17**, 583 (2021).
- [45] F. Zeller, E. Berquist, E. Epifanovsky, and T. Neudecker, *J. Chem. Phys.* **157**, 184802 (2022).
- [46] R. Cammi and B. Chen, *J. Chem. Phys.* **157**, 114101 (2022).
- [47] R. Burden, J. Faires, and A. Burden, *Numerical Analysis* (Cengage Learning, Boston, 2015).
- [48] C. Froese-Fischer, T. Brage, and P. Johnsson, *Computational Atomic Structure: An MCHF Approach* (Taylor & Francis, London, 1997).
- [49] G. C. E. Becker and J. Oden, *Finite Elements. An Introduction* (Prentice-Hall, Englewood Cliffs, 1981).
- [50] T. J. Rivlin, *The Chebyshev Polynomials, Pure and Applied Mathematics* (Wiley-Interscience, New York, 1974).
- [51] J. Gorecki and W. Byers-Brown, *J. Phys. B* **21**, 403 (1988).
- [52] A. F. Duarte-Alcaráz, M. A. Martínez-Sánchez, M. Rivera-Almazo, R. Vargas, R. A. Rosas-Burgos, and J. Garza, *J. Phys. B* **52**, 135002 (2019).
- [53] Y. Yakar, B. Çakır, C. Demir, and A. Özmen, *Phys. Lett. A* **466**, 128724 (2023).
- [54] G. S. T. de Morais and R. Custodio, *J. Mol. Model.* **27**, 212 (2021).
- [55] N. Aquino, J. Garza, A. Flores-Riveros, J. F. Rivas-Silva, and K. D. Sen, *J. Chem. Phys.* **124**, 054311 (2006).
- [56] M. Cinal, *J. Math. Chem.* **58**, 1571 (2020).
- [57] T. Kato, *Commun. Pure Appl. Math.* **10**, 151 (1957).
- [58] E. Clementi and C. Roetti, *At. Data Nucl. Data Tables* **14**, 177 (1974).
- [59] C. F. Bunge, J. A. Barrientos, A. V. Bunge, and J. A. Cogordan, *Phys. Rev. A* **46**, 3691 (1992).
- [60] T. Koga, H. Tatewaki, and A. J. Thakkar, *Theor. Chim. Acta* **88**, 273 (1994).